

# Coherent brightness modulations in the dwarf nova AT Cancri

**Albert Bruch**

Laboratório Nacional de Astrofísica, Rua Estados Unidos, 154,  
CEP 37504-364, Itajubá - MG, Brazil

**James Boardman**

CBA Wisconsin, Luckydog Observatory, 65027 Howath Road, de Soto, WI 54624, USA

**Lewis M. Cook**

American Association of Variable Star Observers, 1739 Helix Ct. Concord, CA 94518,  
USA

**Michael J. Cook**

CBA Ontario, Newcastle Observatory, 9 Laking Drive, Newcastle, ON L1B 1M5, Canada

**Shawn Dvorak**

AAVSO, Rolling Hills Observatory, 1643 Nightfall Drive, Clermont, FL 34711, USA

**James L. Jones**

CBA Oregon, Jack Jones Observatory, 22665 Bents Road NE, Aurora, OR 97002, USA

**John W. Rock**

CBA Wilts, 2 Spa Close, Highworth, Swindon, SN6 7PJ, UK

**Geoffrey Stone**

CBA Sierras, Sierra Remote Observatories, 44325 Alder Heights Road, Auberry, CA  
93602, USA

**Joseph H. Ulowetz**

CBA Illinois, Northbrook Meadow Observatory, 855 Fair Lane, Northbrook, IL 60062,  
USA

(Published in: *New Astronomy*, Vol. 66, p. 22 – 28 (2019))

## Abstract

Light curves of the Z Cam type dwarf nova AT Cnc observed during standstill in 2016 and 2018 are analyzed. On the time scale of hours, previous reports on periodicities, in particular the presence of negative superhumps, could not be confirmed. Instead, a modulation with a period equal to the spectroscopic orbital period was detected which we thus interpret as a manifestations of the binary revolution. It enables us to derive a more accurate value of  $0.201634 \pm 0.000005$  days (or its alias of  $0.021580$  days) for the period. AT Cnc also exhibits a hitherto unreported modulation of  $25.731 \pm 0.005$  min, stable in period but not in amplitude over the entire time base of two years of the observations. We tentatively interpret this modulation in the context of an intermediate polar model for the system.

Keywords: Stars: binaries: close – Stars: novae, cataclysmic variables – Stars: individual: AT Cnc

# 1 Introduction

Cataclysmic variables (CVs) are among the most variable objects in the sky. They exhibit variations of their brightness at practically all wavelengths and on time scales ranging from seconds to millennia. Almost all of these are directly or indirectly caused by mass transfer from a low mass late type star (the secondary) to a more massive white dwarf (the primary) in close orbit around each other. For an exhaustive introduction to our understanding of CVs see, e.g., Warner (1995).

In the majority of these systems, unless the white dwarf has a strong magnetic field which guides mass directly to its surface, the transferred matter first forms an accretion disk around the more massive star where it loses angular momentum and can then settle down on the central object. It is thought that depending on the detailed conditions this disk can switch between a low viscosity and low brightness state termed quiescence with little mass accretion on the white dwarf, and a high viscosity state which permits dumping much of its matter onto the star in a short time. A detailed review of this so-called disk-instability model is given by Lasota (2001). The release of gravitational energy during this process then causes a brightening of the system of several magnitudes (i.e., an outburst) which can last from a few days to a couple of weeks. These systems are known as dwarf novae. A small subgroup of them can remain occasionally in an intermediate state between a full-fledged outburst and quiescence. Such states are termed standstills. After their prototype, the CVs belonging to this subgroup are called Z Cam stars (Buat-Ménard et al. 2001, Simonsen et al. 2014).

One of these is AT Cnc, originally detected as a variable star by Romano & Perssinotto (1968). The early history of the system is summarized by Nogami et al. (1999) to whom the reader is referred for details. The long term light curve is quite well documented in a series of short communications in particular by Meinunger (1981) and Goetz (1983, 1985, 1986, 1988a, 1988b, 1990, 1991). From the 1980s on AT Cnc has also been extensively monitored by amateur astronomer as is testified by its decades long light curve stored in the American Association of Variable Star Observers (AAVSO) International Database<sup>1</sup>. Like many other Z Cam stars, AT Cnc is a very active system which remains hardly ever in quiescence but exhibits a rapid succession of outbursts, sometime interrupted by standstills. Shara et al. (2012) detected a shell around the system, i.e., the remnant of a nova eruption which occurred three or four centuries ago (Shara et al. 2017).

While the long term behaviour of the star is thus well known, more detailed studies of AT Cnc are rare. Only Nogami et al. (1999) published time resolved spectroscopic observations, obtained during a standstill. They measured an orbital period of  $P_{\text{orb}} = 0.2011 \pm 0.0006$  d ( $4.83 \pm 0.01$  h). They also tried to determine the primary star mass ( $M_1 = 0.9 \pm 0.5M_{\odot}$ ), but the large error causes it to be hardly of any use. The orbital inclination is definitely low. Depending on the origin of the  $H\alpha$  emission line Nogami et al. (1999) obtained either  $17^\circ \pm 3^\circ$ , if the emission comes from the secondary star, or  $36^\circ \pm 12^\circ$  if it arises in the accretion disk. The spectrum also exhibits the Na I D absorption lines. This would normally be attributed to an imprint of the secondary star. If AT Cnc would have been in quiescence this would not be surprising considering the rather long orbital period. But this interpretation is less obvious during a standstill. The radial velocity variations of the emission and absorption lines are in phase. If the Na I lines really come from the secondary, this would strengthen the case of the  $H\alpha$  emission to arise from the same source. But the width of  $H\alpha$  emission lines from the secondary, when seen in CVs, is in general quite small, in contrast to what is seen in AT Cnc (see Fig. 7 of Nogami et al. 1999). Moreover, the  $H\alpha$  emission has a P Cyg profile, indicating the presence of absorbing

---

<sup>1</sup><https://www.aavso.org>

material in the system which may also cause the Na I absorption. The Na D lines in the spectrum of AT Cnc are thus not necessarily caused by the secondary star. In a similar case, Ratering et al. (1993) observed Na D absorption in outburst spectra of another Z Cam star, KT Per, during outburst, but not in quiescence. A further example is the SW Sex star PX And (Thorstensen et al. 1991). Finally, Smith (1997) also saw Na D absorption in their spectrum of AT Cnc observed during standstill, but noted the absence of TiO bands which might be expected to be visible if the Na-D lines were due to the secondary star. Thus, the origin of the H $\alpha$  emission and the Na D absorption remains open.

Nogami et al. (1999) also obtained a limited amount of time resolved photometric observations. They found indications for the presence of low amplitude variations with a possible period of 0.249 or 0.132 d (or aliases thereof) in their light curves. This is different from a period of 0.239 d claimed to be present in AT Cnc by Goetz (1986) and none is close to the orbital period. A somewhat more extensive set of photometric observations, also obtained during standstill, was presented by Kozhevnikov (2004). He could not confirm the variations found by Goetz (1986) and Nogami et al. (1999) but, separating his data into two sets adjacent in time, he instead finds indications for quasi periods of 4.65 and 4.74 h, slightly less than the spectroscopic orbital period, with amplitudes of 5 – 9 mmag. He interprets these variations as negative superhumps, i.e., caused by brightness variations due to the nodal precession of an accretion disk which is inclined with respect to the orbital plane of the binary system. Kozhevnikov (2004) also detected a broad hump at frequencies of 0.4 – 0.7 mHz (corresponding to periods between  $\sim$ 25 – 40 min) in the power spectra of his light curves.

Here, we investigate additional light curves of AT Cnc in order to address the question of the presence or not of consistent variations in the system. In Sect. 2 the data are presented. In Sect. 3 we look for variations on the orbital time scale, not finding any indication for the presence of superhumps, but a modulation which permits to refine  $P_{\text{orb}}$ . In Sect. 4 we show the presence of a coherent 26.7 min variation. Finally, our results are discussed in Sect. 5 and briefly summarized in Sec. 6.

## 2 Observations

The data used here were all obtained during two episodes of standstill in AT Cnc in 2016, February – April and 2018, March – April. They consist of a total of 37 light curves observed in the Johnson  $V$  band or in white light and then reduced to  $V$  at a variety of small observatories of the Center of Backyard Astrophysics network<sup>2</sup>. The multiple instruments and data reduction procedures imply that the magnitude scale may differ from one data set to the other. However, only relative magnitude measurements are relevant here. Thus, the scale differences are of no consequence. Moreover, several comparison and check stars have been used to determine the magnitude of AT Cnc. This practically eliminates the risk to confound variations in a comparison star with those of the target star (Kozhevnikov 2003, 2007). A list of the employed light curves is given in Table 1. The AAVSO long term light curve encompassing the observing seasons from 2016 – 2018 is shown in Fig. 1. The red dots represent the data used for the present study. All light curves are available at the AAVSO International Database.

The data analysis was performed using the MIRA software system (Bruch 1993). In particular, timing analysis of the data employing Fourier techniques was done using the Lomb-Scargle algorithm (Lomb 1976, Scargle 1982, Horne & Baliunas 1986), well suited for non-equidistant data. The terms “power spectrum” and “Lomb-Scargle periodogram” are

---

<sup>2</sup><https://cbastro.org>

Table 1: Journal of observations

Date	Time (UT)		Number of integrations	Time resol. (sec)	Oscillation*	Observer
	Start	End				
2016 Feb 18	0:26	4:47	187	74	-	J. Ulowetz
2016 Feb 19	1: 4	3:52	144	71	-	S. Dvorak
2016 Feb 23	2:53	11:15	675	44	+	J. Jones
2016 Feb 26	2:59	6: 4	252	44	+	J. Jones
2016 Feb 27	1:21	6: 5	222	75	+	J. Boardman
2016 Feb 28	0:29	8:15	333	74	+	J. Ulowetz
2016 Mar 2	1:15	5:38	212	74	+	J. Boardman
2016 Mar 3	0: 2	6:46	234	99	+	K. Menzies
2016 Mar 4	5: 8	7:56	111	74	+	J. Ulowetz
2016 Mar 11	1:40	6:57	254	75	o	J. Boardman
2016 Mar 12	0:46	7:25	300	74	+	J. Ulowetz
2016 Mar 17	3:21	9:50	448	44	-	J. Jones
2016 Mar 21	2:44	6:50	183	74	o	J. Ulowetz
2016 Apr 5	4: 4	7:38	325	35	+	L. Cook
2018 Mar 6	3:15	9:24	450	44	o	G. Stone
2018 Mar 7	3:18	9:14	418	45	+	G. Stone
2018 Mar 8	3:22	9:12	331	51	o	G. Stone
2018 Mar 8	20:42	23:27	263	36	-	J. Rock
2018 Mar 10	19:47	22:27	249	36	-	J. Rock
2018 Mar 11	19:19	22:52	166	69	-	D. Barrett
2018 Mar 12	0:30	3:28	148	73	o	M. Cook
2018 Mar 13	19:12	24: 9	476	36	-	J. Rock
2018 Mar 17	0:31	6:50	428	50	+	S. Dvorak
2018 Mar 18	0:31	6:30	407	51	+	S. Dvorak
2018 Mar 19	0:30	5:33	302	52	+	S. Dvorak
2018 Mar 19	19:14	22: 2	176	37	+	J. Rock
2018 Mar 20	0: 5	4:56	238	73	+	M. Cook
2018 Mar 21	0:47	6:35	395	51	-	S. Dvorak
2018 Mar 21	19:24	21:28	200	36	-	J. Rock
2018 Mar 23	1:46	5:27	326	40	+	S. Dvorak, J. Boardman
2018 Mar 24	0:36	3:35	172	50	-	S. Dvorak
2018 Apr 2	1:44	6:34	381	44	o	J. Boardman
2018 Apr 7	1:51	6:11	351	44	+	J. Boardman
2018 Apr 8	1:51	6:12	346	45	+	J. Boardman
2018 Apr 12	1:21	5:10	255	50	+	S. Dvorak
2018 Apr 13	1:37	5: 5	233	51	+	S. Dvorak
2018 Apr 14	1:25	4:60	224	50	+	S. Dvorak

\*: + = definitely present  
o = probably present  
- = absent

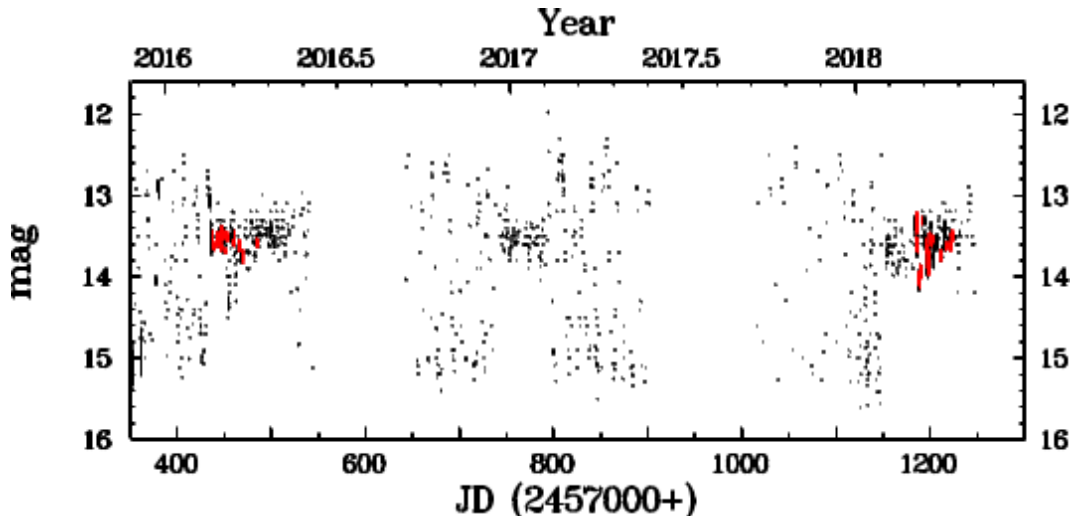


Figure 1: AAVSO light curve of AT Cnc encompassing the observing seasons from 2016 to 2018. The data used in the present study are shown in red. (For interpretation of the references to colour in this figure legend, the reader is referred to the web version of this article.)

used synonymously hereafter. Whenever light curves from different nights were combined, the barycentric correction was applied to the time information, using the on-line tool of Eastman et al. (2010), in order to remove light travel effects in the solar system.

### 3 Orbital variations

The light curves of AT Cnc exhibit variations on the time scale of hours. However, regarding them individually, no consistent common time scale is apparent. Formal fits of simple sine functions yield widely varying periods. In Fig. 2 we plot representative light curves from four nights, each covering a time base of approximately the orbital period. While significant variations on time scales of several hours are clearly present, at most the observations of 2016, March 11 and 2018, March 17 suggest a repeatable pattern.

In order to investigate the question of consistent variations on this time scale further, we combined the light curves into two data sets, one for each of the two observing seasons. Before doing so, we subtracted the average magnitude of each light curve in order to remove night-to-night variations and differences of the magnitude scales caused by the variety of instruments used for the observations. A Lomb-Scargle periodogram was then calculated from the resulting seasonal light curves.

These power spectra are plotted in the left frames Fig. 3 as black graphs. The uneven time distribution of the light curves gives rise to a very complicated pattern of peaks, caused by aliasing effects and possibly the presence of multiple periods or quasi-periods. Comparing the periods corresponding to the most prominent peaks to those mentioned by Goetz (1986), Nogami et al. (1999) and Kozhevnikov (2004), we find only one of them, in 2018, to be close to the 0.249 day period claimed by Nogami et al. (1999). The difference between their and our period value is only 2.1 min. The period error in our data is 0.8 min as judged from the standard deviation of a Gaussian fit to the respective power spectrum peak. Nogami et al. (1999) provide no error estimate, but it should even be larger considering the short

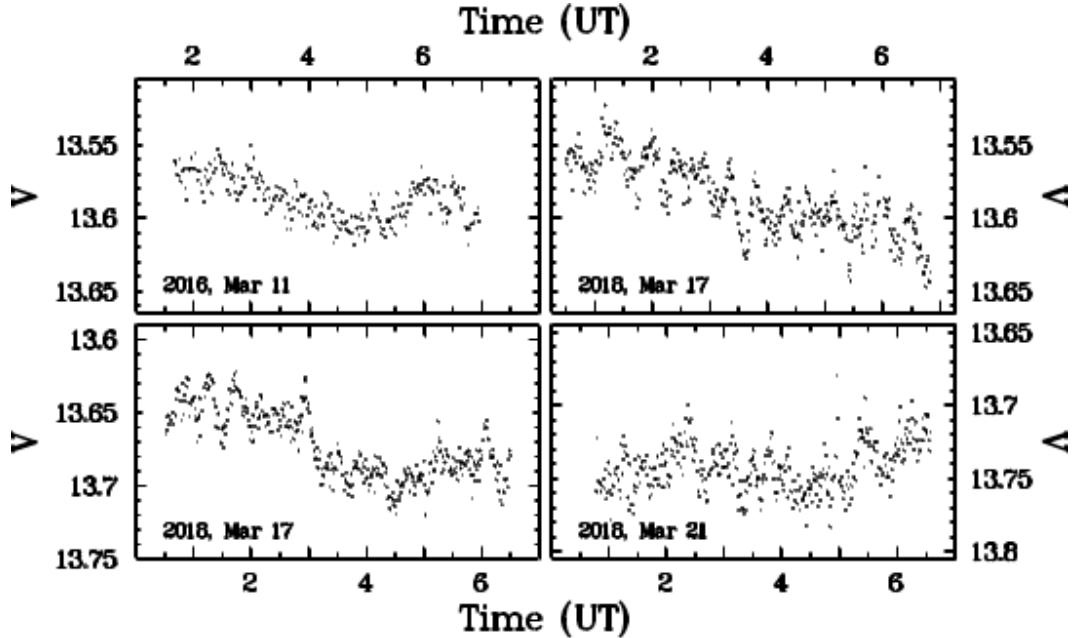


Figure 2: Some representative nightly light curves of AT Cnc, all plotted on the same time and magnitude scale.

time base of their observations. Therefore, the difference is insignificant. There may thus be some evidence that during 2018 a similar modulation as seen by Nogami et al. (1999) in 1997 was present, but it cannot be considered sufficient to claim a definite detection (see also below).

In an effort to clean the complex power spectra from alias and window effects, we applied the CLEAN algorithm (Roberts et al. 1987) to the data. The cleaned power spectra are superposed upon the Lomb-Scargle periodograms as red graphs in Fig. 3. While this procedure is not perfect (some maxima in the resulting spectra can still readily be identified as being caused by the window function<sup>3</sup>), the cleaned spectra are much easier to interpret. As an aside we first mention that the maximum corresponding to the period claimed by Nogami et al. (1999) (which should be at 0.168 cycles/hour) has vanished, casting doubts on the reality of this modulation.

More important is, however, the survival of only one significant peak common to the data sets of both years. A blown-up view of the Lomb-Scargle periodogram of a small frequency interval around this peak is plotted in the central frames of Fig. 3 and shows the perfect alignment of the signals. The average of the corresponding periods in the two seasons is 4.839 h. Within the error bars quoted by Nogami et al. (1999) it is identical to the spectroscopic orbital period, lending credibility to the reality of this photometric period which we will henceforth identify with  $P_{\text{orb}}$ . The formal error is only 0.00003 h if it is taken as the standard deviation of the two independent period measurements of 2016 and 2018. This may be an underestimate. If we take instead the standard deviation of a Gaussian fit to the corresponding peak in the power spectra the error increases to 0.008 h. Folding the light curves on  $P_{\text{orb}}$ , choosing the epochs such that the minimum coincides with phase 0,

<sup>3</sup>The highest peak in the 2018 power spectra corresponds, e.g., to a period of exactly 12 h and is thus very likely an effect of data sampling.

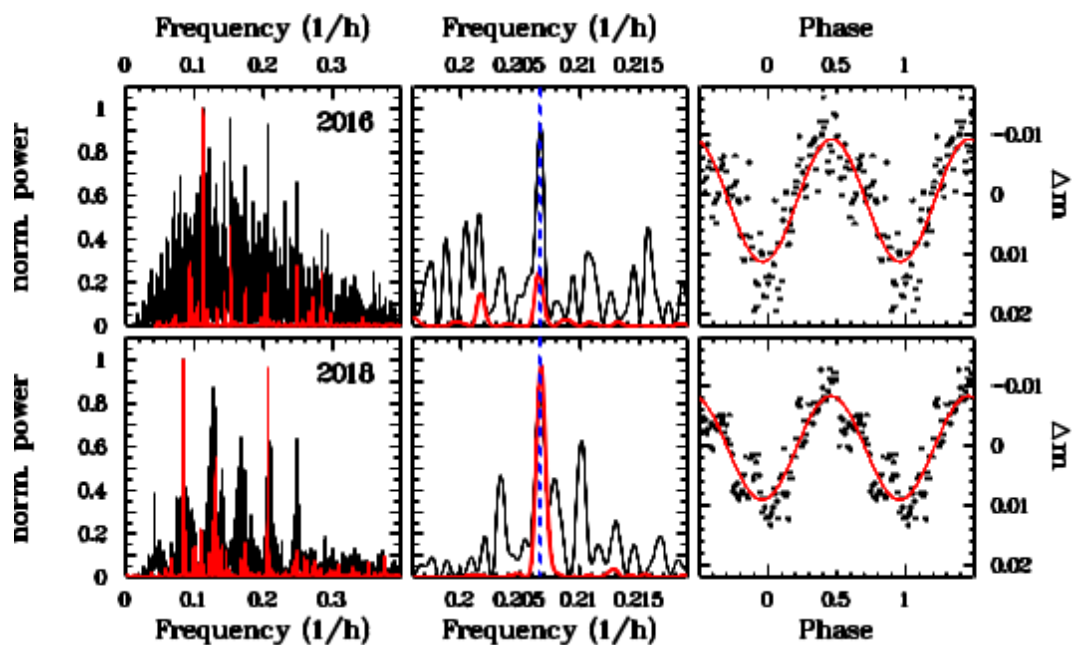


Figure 3: Analysis of variations in AT Cnc occurring on the time scale of several hours. *Left:* Lomb-Scargle periodograms of the combined light curves of 2016 (top) and 2018 (bottom), normalized to the power of the highest peak. The cleaned power spectra are over plotted in red. *Center:* The same periodograms as shown in the left frame, restricted to a narrow range around the frequency corresponding to the orbital period. The broken vertical line indicates the average of these frequencies measured in the two observing seasons. *Right:* The combined light curves, folded on the period of the highest peak in the central frames, binned in phase bins of width 0.01. The red curves are the best sine fits. (For interpretation of the references to colour in this figure legend, the reader is referred to the web version of this article.)

results in graphs plotted in the right frames of Fig. 3. The best fit sine curve is also shown (in red). Note that it is not a perfect fit, leaving systematic residuals at maximum and minimum phases. Thus, not unexpectedly, the orbital variations are more complex than a simple sine wave. At 20.2 mmag in 2016 and 17.4 mmag in 2018 the total amplitude of the sine curves and thus the amplitude of the variations are similar in both years.

Adopting the more conservative error limit of 0.008 h for  $P_{\text{orb}}$  leads to a cycle count uncertainty of  $\sim 1.2$  between the two observing seasons. Thus, it is not possible to unambiguously connect both data sets. The period can be expressed as  $\Delta T/E$ , where  $\Delta T$  is the time difference between two minima in the light curve and  $E$  is an integer values, indicating the number of elapsed cycles. Let  $\Delta T = 747.459$  days be the time difference of the epochs chosen to calculate the phase folded light curves in the right frames of Fig. 3. Then only  $E = 3707$  or  $E = 3708$  lead to periods which are compatible within its errors with the preliminary period quoted above. This implies that either  $P_{\text{orb}} = 0.201634$  d (4.83922 h) or  $P_{\text{orb}} = 0.201580$  d (4.83792 h).

Using as a conservative criterion for the uncertainty of these values the condition that it must not lead to a phase difference of more than 10% over the time interval  $\Delta T$ , the period error is 0.0000054 d (0.00013 h). The minimum epoch is  $\text{BJD}_{\text{min}} 2458184.975 \pm 0.020$ , where the error was again chosen such that a maximum phase error of 10% is permitted.

## 4 A coherent 26.7 min variation

As can be seen in Fig. 2, variations on shorter time scales are superposed upon the modulations occurring on the time scale of hours. At first glance they appear to the eye as irregular flickering, a common feature in all CVs (Bruch 1992). However, in some cases there seems to be a certain regularity. Indeed, regarding the respective frequency range of the Lomb-Scargle periodograms of the individual nightly light curves we find that in many of them not only significant signals at frequencies corresponding to the periodicity of the apparent variations occur, but – more so – that they always appear at the same frequency of  $\sim 2.25$  cycles/hour. In anticipation of the interpretation of these variations in Sect. 5 we will call the period corresponding to this frequency the rotational period  $P_{\text{rot}}$  and thus find  $P_{\text{rot}} = 26.7$  min. The average frequencies measured during the two observing seasons of 2016 and 2018 are identical within their respective standard deviations. Thus, these light changes should not be regarded as some quasi-periodicity, but as a coherent modulation of the light of AT Cnc. In the last but one column of Table 1 a plus sign (“+”) indicates those light curves which definitely exhibit the signal in their power spectra, while a minus sign (“−”) is assigned to those lacking it. A “o” marks the cases, where a weak signal is present at the corresponding frequency which, however, would not be regarded as significant by itself (i.e., without expecting it to be present). Fig 4 shows three examples of light curves (upper frames) and their corresponding Lomb-Scargle periodograms (lower frames).

In order to test the stability of  $P_{\text{rot}}$  and to get a more precise numerical value, those light curves which strongly exhibit the corresponding signal, were combined into a single data set, separately for the two observing season. In this case, and differently from the procedure adopted in Sect. 3, not only the average magnitude of the individual light curves was subtracted in order to remove night-to-night variations and differences of the magnitude scales, but a polynomial of suitable order was fit and subtracted from each of them in order to reduce low frequency noise. The resulting combined light curves were then again submitted to a frequency analysis.

The result is convincing and is shown in Fig. 5. The left frames show the power spectra for 2016 (top) and 2018 (bottom). Again, both contain a complicated pattern of peaks which is



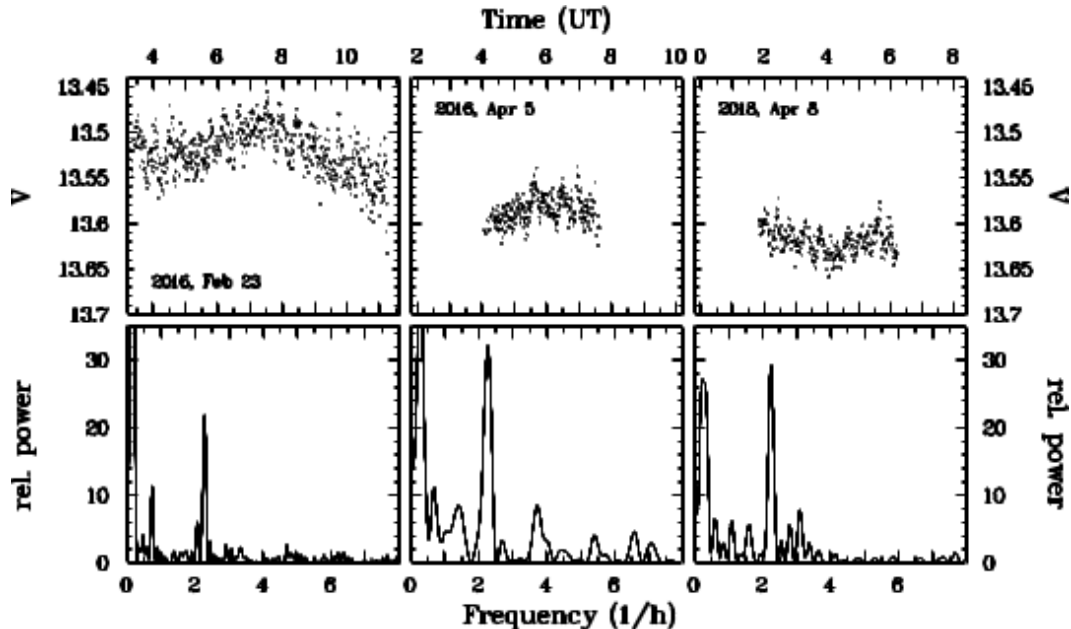


Figure 4: *Upper frames*: Three representative light curves of AT Cnc, all drawn on the same magnitude and time scale. *Lower frames*: Lomb-Scargle periodograms of the light curves shown in the upper frames, also drawn on the same scale.

to be expected considering the uneven time distribution of the individual contributing light curves. Considering the most significant maxima, there is only one coincidence between the two observing season: The highest peak in 2016 is well aligned with the second highest peak in 2018. This becomes even clearer regarding the central frames of the figure which contain blown-up versions of the power spectra, restricted to a narrow frequency interval around the two peaks. The blue vertical lines, which corresponds to the mean of the frequency maxima of the two peaks, clearly reveals their excellent alignment<sup>4</sup>. We take the standard deviation of a Gaussian fit to the peaks as a conservative measure of the frequency error. Then  $P_{\text{rot}} = 26.731 \pm 0.005$  min. The combined light curves, folded on this period and binned in phase intervals of width 0.01 are plotted in the right frames of Fig. 5. They can be well represented by an sine wave, and the red curve in the figure represents the best fit sine curve which has a full amplitude of 17.8 mmag in 2016 and 9.4 mmag in 2018. Again, the epoch has been chosen such that the minimum coincides with phase 0, independently for 2016 and 2018.

The error of  $P_{\text{rot}}$  is too large to permit a reliable cycle count between the two observing seasons. Over the  $\sim 2$  years between them the ambiguity sums up to  $\sim 7.5$  cycles. Therefore, we can only say that  $P_{\text{rot}} = \Delta T / (E + n)$ , where  $\Delta T$  is the time difference between the observations, the integer value  $E$  is an estimate for the elapsed number of cycles, and  $n$  is the error of  $E$ , also expressed as an integer value. Using  $\Delta T = 743.083$ , i.e., the difference of the epochs used to calculate the folded light curves in the right frames Fig. 5, together the preliminary value of  $P_{\text{rot}}$  as quoted above gives a best estimate of  $E = 40029$ . Then,  $P_{\text{rot}} = 26.73161 \pm 0.00007$  min, where the error was defined such as to permit a maximum

<sup>4</sup>The satellite peak to the right of the main peak in 2016 can be explained as an alias caused by the window function.

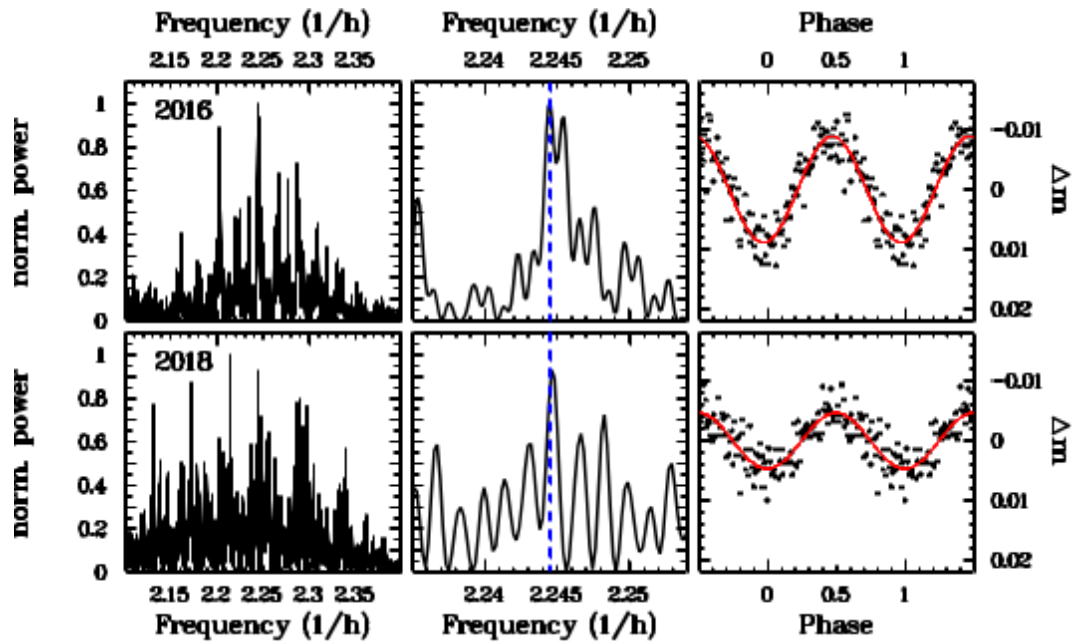


Figure 5: Analysis of the 26.7 min variation in AT Cnc. *Left:* Lomb-Scargle periodograms of the combined light curves of AT Cnc of 2016 (top) and 2018 (bottom), normalized to the power of the highest peak. *Center:* The same periodograms as shown in the left frame, restricted to a narrow range of frequencies around the frequency of the highest peak in the 2016 periodogram. The broken vertical line corresponds to the average of the frequencies of the highest peaks in the both years. *Right:* The combined light curves, folded on the period of the highest peak in the central frames, binned in phase bins of width 0.01. The red curves are the best sine fits to the data. (For interpretation of the references to colour in this figure legend, the reader is referred to the web version of this article.)

phase error of 10% between the observing seasons. Remember, however, that the true period may well be an alias of this value!

## 5 Discussion

### 5.1 The orbital period

This investigation has revealed two consistent periods in the light curves of AT Cnc which were observed in two observing seasons separated by two years. The first of them lies within the error limits of the previously determined spectroscopic orbital period. We therefore identify it as a manifestation of orbital variations. The error of the photometric period is smaller than that of the spectroscopic one. Thus, the revolution period of AT Cnc could be determined with a higher accuracy, which, however, is unfortunately not high enough to permit an unambiguous cycle count between 2016 and 2018 and thus to increase the accuracy by another order of magnitude.

The amplitude of the orbital variations is only of the order of 0.01 mag, significantly smaller than the total range of variations seen in individual nightly light curves. These are thus dominated by modulations which must have other origins and which we will not explore in more detail here. We only mention that this behaviour is not uncommon in cataclysmic variables. Orbital variations in CVs are in general attributed to the changing visibility of structures in the accretion disk as – in a frame of reference fixed in the binary system – the line of sight to the observer changes. The accretion disk being largely a two-dimensional entity aligned to the orbital plane, this effect should decrease with decreasing orbital inclination of the system. Nogami et al. (1999) have shown that we see AT Cnc more or less along the axis of the binary revolution. This is in line with the small amplitude of the orbital modulations.

Apart from  $P_{\text{orb}}$  no other convincing persistent periodicity on the time scale of hours could be seen in our data. Therefore, it can be concluded that all other periodic variations in the light curves of AT Cnc as seen by Goetz (1986), Nogami et al. (1999) and Kozhevnikov (2004) are transient features. In particular, the negative superhumps claimed by Kozhevnikov (2004), if real, do not persist over time.

### 5.2 The 26.7 min period

The second consistent periodicity found here,  $P_{\text{rot}}$ , is a coherent oscillation with a period of about half an hour. It is doubtful if it can be associated to the broad hump at frequencies of 0.4 – 0.7 mHz which Kozhevnikov (2004) saw in his average power spectrum. The period coincides with the upper limit of this frequency range, but in the present data  $P_{\text{rot}}$  causes a sharp peak in the power spectra, not a broad hump. Moreover, the individual power spectra shown in Fig. 3 of Kozhevnikov (2004) do not contain this peak. Two mechanisms come to mind to explain the 26.7 min modulation: white dwarf oscillations or white dwarf rotation. We will consider these possibilities in turn.

#### 5.2.1 White dwarf oscillations

White dwarf oscillations are not commonly seen in CVs, but they are not unprecedented. The first and (to our knowledge) so far only confirmed case is the WZ Sge type dwarf nova GW Lib. The white dwarf in this system exhibits non-radial oscillations (van Zyl et al. 2000, 2004) otherwise observed in some isolated white dwarfs of type DA, i.e., the ZZ Cet stars.

However, an interpretation of the 26.7 min oscillation in AT Cnc in this way has a number of difficulties. To begin with, the period is longer than any found in the comprehensive list of ZZ Cet star characteristics of Kepler (2016). Moreover, ZZ Cet stars often exhibit more than one period. In light curves obtained in several years, GW Lib, for example, routinely exhibits two or three periods (disregarding the fine structure in the respective power spectra; van Zyl et al. 2000) which are not absolutely stable. In contrast, only a single oscillation period is found in AT Cnc, at a stable frequency in all observations obtained so far.

The oscillation amplitude in ZZ Cet stars range from a few milli-magnitudes to a couple of centi-magnitudes (Kepler 2016). While this is compatible with the amplitudes seen in AT Cnc, those values hold for naked white dwarfs. But in a CVs the oscillations will be diluted by the light from the accretion disk. The observed amplitudes in GW Lib as observed by van Zyl et al. (2000) range between 14.5 mmag and 1.9 mmag, with values above 10 mmag being rare. This is not unlike what is seen in AT Cnc. However, in a short period WZ Sge star in quiescence the accretion disk is expected to be rather faint such that the white dwarf light contributes significantly to the total visual light. AT Cnc at standstill and with a much longer orbital period will have a much brighter accretion disk. Thus, for the observed oscillation amplitude to reach almost 20 mmag, the intrinsic amplitude must be much higher<sup>5</sup>.

Finally, the white dwarfs in dwarf novae above the period gap all have surface temperatures well in excess of 20 000 K (Sion 2012). This is much beyond the empirical range of  $\sim 11\,000$  K to  $\sim 12\,000$  K (Van Grootel et al. 2012) of the instability strip within which ZZ Cet type oscillations can occur.

All these arguments speak against an origin of the 26.7 min period as an oscillation of the white dwarf in AT Cnc.

### 5.2.2 White dwarf rotation

The second mechanism to explain the 26.7 min oscillation is rotation of the white dwarf in the framework of an intermediate polar (IP) model for AT Cnc. In such systems the white dwarf has a substantial magnetic field which is able to disrupt the inner accretion disk and guide matter via a curtain shaped structure to the magnetic poles, generating bright spots on the compact star. The varying aspect of these spots as the white dwarf rotates together with self occultations by the body of the white dwarf and absorption by (parts of) the accretion curtain modulates the observed light as the star rotates.

In many IPs the ratio of the white dwarf rotation period to the orbital period is close to 0.1 (Barrett et al. 1988, Warner & Wickramasinghe 1991). King (1991) show that this is the consequence of an equilibrium configuration naturally assumed by IPs if the white dwarf essentially accretes the specific angular momentum of the secondary star. In the present case we find  $P_{\text{rot}}/P_{\text{orb}} = 0.092$ , in excellent agreement. In the left frame of Fig. 6 the location of all confirmed IPs listed on K. Mukai’s IP home page<sup>6</sup> in the  $P_{\text{orb}} - P_{\text{rot}}$  plane is plotted (neglecting the long orbital period system GK Per). The solid, dashed and dotted black lines represent  $P_{\text{rot}}/P_{\text{orb}}$  ratios of 0.1, 0.5, and 0.01, respectively. The red lines (again in the sequence solid, dashed and dotted) embody the spin equilibrium condition according to Eq. 10 of King (1991) for mass ratios of  $q = M_2/M_1 = 1, 0.5, \text{ and } 0.1$ , respectively. Here,

<sup>5</sup>A hand waving argument, assuming that the white dwarf and the accretion disk have the same brightness in a system with an orbital period of 1.5 h, using typical CV component masses and Kepler’s law to scale the system dimensions (and thus the disk surface) to the period of AT Cnc, and considering the higher disk luminosity at standstill, shows that the intrinsic oscillation amplitude of the white dwarf must then be of the order of 0.5 mag, an order of magnitude higher than any amplitude observed in a ZZ Cet star.

<sup>6</sup><https://ads.gfsc.nasa.gov/Koji.Mukai/iphome/iphome.html>; we use all confirmed and “ironclad” systems in Mukai’s notation.

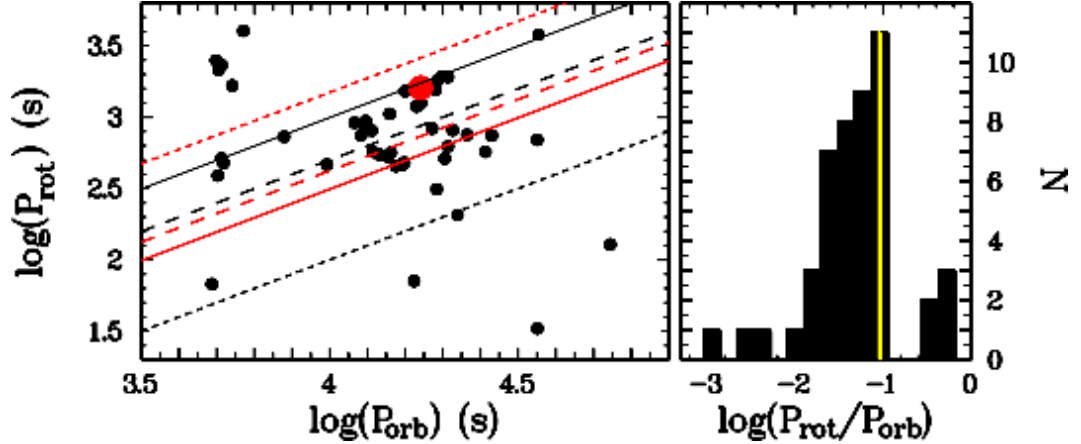


Figure 6: *Left:* Location of confirmed intermediate polars in the  $P_{\text{orb}} - P_{\text{rot}}$  plane. The location of AT Cnc is indicated as a red dot under the assumption that the 26.7 min oscillation represents the rotation period of the white dwarf. The solid, dashed and dotted black lines represent  $P_{\text{rot}}/P_{\text{orb}}$  ratios of 0.1, 0.5, and 0.01, respectively. The red lines (solid, dashed and dotted) embody the equilibrium condition according to Eq. 10 of King (1991) for mass ratios of 1, 0.5, and 0.1, respectively. *Right:* The distribution of the logarithms of the  $P_{\text{rot}}/P_{\text{orb}}$  ratio of confirmed intermediate polars. The location of AT Cnc is indicated as a yellow vertical line. (For interpretation of the references to colour in this figure legend, the reader is referred to the web version of this article.)

$M_1$  and  $M_2$  are the masses of the white dwarf and the secondary star. The location of AT Cnc is indicated by a red dot and is very well aligned with numerous other intermediate polars. This is also evident in the right frame of Fig. 6, which contains a histogram of the (logarithmic)  $P_{\text{rot}}/P_{\text{orb}}$  ratios. AT Cnc, indicated by a yellow vertical line, falls right on the peak of the distribution.

The power spectra of some IPs exhibit signals at the orbital side bands of the white dwarf rotation frequency. (e.g., TX Col, Buckley & Tuohy 1989; AO Psc, Hellier et al. 1991). These may be caused by reprocessing of radiation from the emission regions on the white dwarf in a region fixed in the orbital frame of reference. Our periodograms contain signals at  $2.4514 \text{ h}^{-1}$  (2016) and  $2.4508 \text{ h}^{-1}$  (2018). This is close to  $1/P_{\text{rot}} + 1/P_{\text{orb}} = 2.4512 \text{ h}^{-1}$ . While they may thus be positive orbital sidebands, they are weak and it would be premature to definitively identify them as such.

The amplitude of the  $P_{\text{orb}}$  variations is small compared to what is observed in most IPs (except the small subset of IPs named DQ Her stars, where the white dwarf rotation period is less than  $\sim 2$  min; see chapter 8 of Warner, 1995). This may be due to the low orbital inclination of AT Cnc: If the magnetic poles are approximately aligned with the rotation axis, we may see only one pole and the aspect of the bright spot on the white dwarf surface may not change much due to rotation. Consequently, the light modulation and thus the amplitude remains small.

The amplitude is, however, much smaller in 2018 than it was in 2016. Since the average system magnitude in both seasons was the same within a few hundredth of a magnitude, this cannot be explained by a brighter accretion disk in 2018 diluting the rotational modulation. Instead, the latter must have been systematically smaller in 2018. The different strength of the respective power spectrum signal in different nights, up to its complete disappearance

also points at significant changes in the flux of the light source causing the modulations. We may speculate about a changing mass accretion onto the white dwarf. Either the accretion decreases to a degree that the bright spot at the visible magnetic pole gets too faint to cause a sufficient modulation of the total light output of the system, or – assuming a weak magnetic field – an increased mass transfer causes the Alfvén radius, i.e., the radius at which the accretion is dominated by the magnetic field, to decrease so much that it becomes smaller than the white dwarf radius or at least small enough such that the foot point of the accretion curtain on the white dwarf becomes too large for significant modulations due to the changing aspect caused by the white dwarf rotation to be seen. However, in both cases this should be accompanied by a change in the system magnitude: in the first case to a lower brightness (decrease of accretion luminosity), in the second case to higher brightness (increase of accretion luminosity). Such a correlation is not obvious in our data.

The lack of observed x-rays from AT Cnc may appear as an obstacle for the interpretation of the system as an intermediate polar because, in general, IPs are copious hard x-ray emitters. In fact, a considerable number of them were first identified through their periodic x-ray modulations. Verbunt et al. (1997) searched the ROSAT XRT-PSPC All Sky Survey for x-rays from 162 CVs with known or detected binary periods. Among them was AT Cnc which was not detected. We are also not aware of any other x-ray observation of the system. However, the sample of Verbunt et al. (1997) contains also such well-known intermediate polars as FO Aqr, BG CMi and DQ Her which were not detected. Therefore, the absence of detected x-rays from AT Cnc in the ROSAT survey may not be a conclusive argument against an IP nature.

## 6 Conclusions

The analysis of 37 light curves of the Z Cam type dwarf nova AT Cnc obtained during two standstills spanning about 7 weeks in 2016 and 6 weeks in 2018, comprising a total of 170 hours of observations, did not confirm the consistent presence of any of the periods on time scales of hours claimed in previous publications. In particular, no indications of superhumps as reported by Kozhevnikov (2004) were detected. In the individual light curves variations with amplitudes of the order of 0.1 mag are common, but they are not obviously regular. However, a power spectrum analysis of the combined light curves of each observing season revealed the presence of a low amplitude ( $\sim 0.02$  mag) modulation with the same period in 2016 and 2018 and equal to within the error margin to the spectroscopic orbital period. It may therefore confidently be regarded as a photometric manifestation of revolution of the binary system. Since the error of this photometric period is smaller than of the previously known spectroscopic one, the binary period of AT Cnc could be determined with a somewhat higher accuracy.

A second, shorter photometric period of  $\sim 26.7$  min is evident in the power spectra of many, albeit not all, light curves in both years. Its stability in frequency is testified by the presence of the same feature in the combined seasonal light curves. While the corresponding power spectra are noisy (in particular in 2016) because of the complicated window spectrum, making it difficult to identify the exact period or to distinguish between one coherent period or several quasi-periods caused by, e.g., quasi-periodic oscillations, one and only one of the significant power spectrum peaks is present at exactly the same frequency in both, 2016 and 2018. Thus, this appears to be a coherent modulation in AT Cnc, stable at least over the time scale of years. We discuss two scenarios for this modulation. An oscillation of the white dwarf as observed in the WZ Sge type star GW Lib can probably be discarded. More promising is an explanation in the context of an intermediate polar model of AT Cnc,

although there may also be problems with this interpretation in view of the presence and absence of the 26.7 min variations in different nights without a substantial change of the system brightness, and the lack of observed x-ray emission.

## Acknowledgements

We gratefully acknowledge the efforts of those AAVSO observers who contributed light curves for this study but are not co-authors, namely D. Barrett and K. Menzies. We also thank the AAVSO as an organization for their excellent work to maintain the International Database which is a treasure trove ready to be exploited.

## References

- Barrett, P., O'Donoghue, D., & Warner, B. 1988, *MNRAS*, 233, 759
- Bruch, A. 1992, *A&A*, 266, 237
- Bruch, A. 1993, *MIRA – A Reference Guide*, Astron. Inst. Univ. Münster
- Buckley, D.A.H., & Tuohy, I.R. 1989, *ApJ*, 344, 376
- Buat-Ménard, V., Hameury, J.-P., & Lasota, J.-P. 2001, *A&A*, 369, 925
- Eastman, J., Siverd, R., & Gaudi, B.S. 2010, *PASP*, 122, 935
- Götz, W. 1983, *IBVS* 2363
- Götz, W. 1985, *IBVS* 2734
- Götz, W. 1986, *IBVS* 2918
- Götz, W. 1988a, *IBVS* 3066
- Götz, W. 1988b, *IBVS* 3208
- Götz, W. 1990, *Mitt. Veränd. Sterne*, 12, 60
- Götz, W. 1991, *Mitt. Veränd. Sterne*, 12, 111
- Hellier, C., Cropper, M., & Mason, K.O. 1991, *MNRAS*, 248, 233
- Horne, J.H., & Baliunas, S.L. 1986, *ApJ*, 302, 757
- Kepler, S.O. 2016, <http://astro.if.ufrgs/zzcet.htm>
- King, A.R., & Lasota, J.-P. 1991, *ApJ*, 378, 674
- Kozhevnikov, V.P. 2003, *A&A*, 398, 267
- Kozhevnikov, V.P. 2004, *A&A*, 419, 1035
- Kozhevnikov, V.P. 2007, *A&A*, 465, 557
- Lasota, J.-P. 2001, *New Astr. Rev.*, 45, 449
- Lomb, N.R. 1976, *Ap&SS*, 39, 447
- Meinunger, L. 1981, *Mitt. Veränd. Sterne*, 9, 59
- Nogami, D., Masuda, S., Kato, T., & Hirata, R. 1999, *PASJ*, 51, 115
- Ratering, C., Bruch, A., & Diaz, M.P. 1993, *A&A*, 268, 694
- Roberts, D.H., Lehár, J., & Dreher, J.W. 1987, *AJ*, 93, 968
- Romano, G., & Persinotto, M. 1968, *Publ. Astr. Obs. Padova*, 151, 9
- Scargle, J.D. 1982, *ApJ*, 263, 853
- Shara, M.M., Drissen, L., Martin, T., Alarie, A., & Stephenson, F.R. 2017, *MNRAS*, 465, 739
- Shara, M.M., Mizusawa, T., Wehinger, P., et al. 2012, *ApJ*, 758, 121

Simonsen, M., Boyd, D., Goff, W., et al. 2014, JAAVSO, 42, 1  
Sion, E.M. 2012, JASS, 29, 169  
Smith, R.C., Sarna, M.J., Catalán, M.S., & Jones, D.H.P. 1997, MNRAS, 287, 271  
Thorstensen, J.R., Ringwald, F.A., Wade, R.A., Schmidt, G.D., & Norsworthy, J.E. 1991, AJ, 102, 272  
Van Grootel, V., Dupret, M.-A., Fontaine, G., et al. 2012, A&A, 439, A87  
van Zyl L., Warner, B., O'Donogue, D., et al. 2000, Baltic Astr., 9, 231  
van Zyl L., Warner, B., O'Donogue, D., et al. 2004, MNRAS, 350, 307  
Verbunt, F., Bunk, W.H., Ritter, H., & Pfeffermann, E. 1997, A&A, 327, 602  
Warner, B. 1995, Cataclysmic Variable Stars, Cambridge University Press, Cambridge  
Warner, B., & Wickramasinghe, D.T. 1991, MNRAS, 248, 370